Experimental Investigation of Clear-Water Local Scour of Compound Piers

B. Ataie-Ashtiani[1]; Z. Baratian-Ghorghi[2]; and A. A. Beheshti[3]

Abstract: Local scour around complex piers under steady clear-water condition was studied experimentally for a variety of configuration, including different sizes and shapes of complex piers. A total of 70 experiments were carried out. Three sets of experiments were performed over the entire range of possible pile cap elevations for complex piers with different geometrical characteristics. The collected data are used to quantify the pile cap elevations that maximize or minimize the local scour depth. Some of the available methodologies to estimate the maximum local scour depth around such complex piers are evaluated. The predictions of the scour depths improved by using the revised methods of *Hydraulic Engineering Circular Number 18* and Coleman.

DOI: 10.1061/(ASCE)0733-9429(2010)136:6(343)

CE Database subject headings: Scour; Bridges; Piers; Pile groups; Foundations.

Author keywords: Local scour; Bridges; Complex piers; Pile cap; Pile group; Foundation.

Introduction

Estimation of the scour depth, y_s, around bridge piers has been studied for many years. Most studies have been performed for bridge piers with a uniform cross section (e.g., Melville and Sutherland 1988; Raudkivi and Ettema 1983; Hannah 1978), but due to geotechnical and economical reasons, multiple-pile bridge piers and complex piers have become popular in bridge design (Parola et al. 1996; Melville and Coleman 2000; Coleman 2005; Ataie-Ashtiani and Beheshti 2006). The complex piers (see Fig. 1) are constructed of several components, i.e., column, pile cap, and pile group, and proper scour prediction is necessary for this kind of foundation.

Melville and Coleman (2000) proposed a procedure to predict y_s at complex piers, involving equations that are used to characterize the different combinations of pier components. This procedure does not consider the existence of pile group below the pile cap. Therefore with complex piers, the estimated y_s increases with increasing pile cap elevation relative to the bed level, Y, as in the columns founded on caissons. Coleman (2005) revised this procedure by considering five different Y and assuming linear variation in y_s. The methodology used the expressions of Melville and Coleman (2000) and the results of Parola et al. (1996) work, and was based on several existing equations, i.e., the equation of single piers, caisson-founded piers, pile groups together with debris rafts, and pile groups alone.

The Federal Highway Administration (FHWA) recommended a superposition method for complex piers in its *Hydraulic Engineering Circular No. 18* (Hec-18) (Richardson and Davis 2001), with y_s being obtained from the sum of various contributions to the scour depth caused by each component

$$y_s = y_{s\text{pier}} + y_{s\text{pc}} + y_{s\text{pg}} \tag{1}$$

where $y_{s\ \text{pier}}$=scour component for the pier stem; $y_{s\text{pc}}$=scour component for pile cap or footing; and $y_{s\ \text{pg}}$=scour depth of the piles exposed to the flow. Each of the components in the equation is calculated from (Richardson and Davis 2001)

$$\frac{y_s}{h} = 2.0K_1K_2K_3K_4\left(\frac{D}{h}\right)^{0.65}(\text{Fr})^{0.43} \tag{2}$$

where h=approach flow depth; D=pier diameter; K_1=shape factor; K_2=angle of attack factor; K_3=dune factor; K_4=correction factor for size of bed material; $\text{Fr}=U/(gh)^{0.5}$=Froude number; g=gravitational acceleration; and U=depth averaged approach velocity.

Sheppard and Glasser (2004) proposed an alternative methodology for estimating design scour depth at these structures, in which a complex pier is represented by a single circular pile with an effective diameter, D^*_{total}, such that

$$D^*_{\text{total}} = D^*_{\text{column}} + D^*_{\text{pc}} + D^*_{\text{pg}} \tag{3}$$

where D^*_{column}=effective diameter of pier; D^*_{pc}=effective diameter of pile cap; and D^*_{pg}=effective diameter of pile group.

Because of the complexity of the scour process, especially at complex piers, it is desirable to examine the validity of the predicting methods using laboratory studies. The main objective of this work is to study experimentally the clear-water local scour at complex piers by obtaining a new set of data and to evaluate and improve the current available methodologies for estimating y_s using the collected data.

---

[1] Professor, Dept. of Civil Engineering, Sharif Univ. of Technology, Tehran, Iran. E-mail: ataie@sharif.ir

[2] Graduate Student, Dept. of Civil Engineering, Sharif Univ. of Technology, Tehran, Iran.

[3] Ph.D. Student, Dept. of Civil Engineering, Sharif Univ. of Technology, Tehran, Iran. E-mail: a_beheshti@mehr.sharif.ir

Note. This manuscript was submitted on August 27, 2007; approved on November 12, 2009; published online on May 14, 2010. Discussion period open until November 1, 2010; separate discussions must be submitted for individual papers. This paper is part of the ***Journal of Hydraulic Engineering***, Vol. 136, No. 6, June 1, 2010. ©ASCE, ISSN 0733-9429/2010/6-343–351/$25.00.

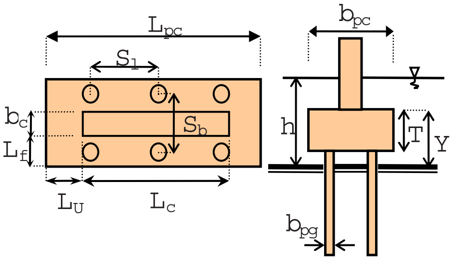

Fig. 1. Complex pier-geometry characteristics

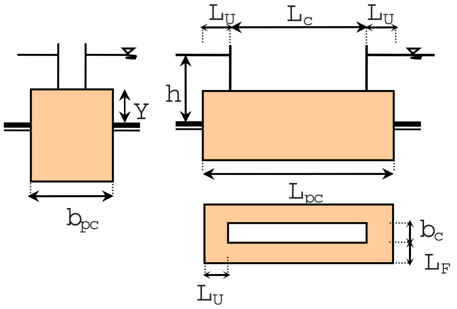

Fig. 2. Caisson-founded pier-geometry characteristics

Dimensional Analysis

The influences of pier, fluid, bed sediments, and fully turbulent flow factors on y_s at a single uniform pier can be expressed functionally as (Ettema et al. 1998; Breusers and Raudkivi 1991)

$$\frac{y_s}{D}=f_1\left(\frac{U}{U_c} \quad \text{or} \quad \text{Fr}, \frac{h}{D}, \frac{d_{50}}{D}\right) \tag{4}$$

where d_{50}=median particle size of the bed sediments and U_c =critical value of U associated with initiation of motion of bed sediments. All of the existing procedures for estimating y_s at complex piers, which will be considered in this study, are based on these nondimensional parameters. The Coleman (2005) and Sheppard and Glasser (2004) procedures both use an equivalent pier width, b_e, in determining y_s from existing equations for single piers. The HEC-18 methodology is different in that b_e is assumed as a function of pier components that are exposed to the flow. Also, in situations where the pile cap is buried or partially buried (see Fig. 3), b_e depends on the sediment and flow properties. Therefore, by using dimensional analysis, a functional relationship may be written for b_e as

$$\frac{y_s}{b_c} \quad \text{or} \quad \frac{b_e}{b_c} = f\left(\frac{U}{U_c} \quad \text{or} \quad \text{Fr}, \frac{h}{b_c}, \frac{b_c}{d_{50}}, \frac{b_c}{b_{\text{pc}}}, \frac{T}{b_{\text{pc}}}, \frac{Y}{b_c}, \frac{L_U}{b_c}, \frac{L_f}{b_c}, k_{\text{sc}}, k_{\text{spc}}, \frac{b_{\text{pg}}}{b_c}, \times m, n, \frac{S_b}{b_{\text{pg}}}, \frac{S_l}{b_{\text{pg}}}\right) \tag{5}$$

in which b_c=column width; b_{pc}=pile cap width; T=thickness of the pile cap; L_U and L_f=extensions of the pile cap upstream of and sides of the column, respectively; k_{sc} and k_{spc}=shape factors for the pier and pile cap (foundation), respectively, as recommended by Melville and Coleman (2000); b_{pg}=pile diameter; m =number of piles inline with flow; n=number of piles normal to the flow; S_l=pile spacing in line with flow; and S_b=pile spacing normal to the flow. The column and pile cap lengths may also be important factors, especially for skewed piers. In this study only aligned flows are considered, hence, shape factors can be assumed to be constant. The large number of variables makes it difficult to consider all of them in limited experiments. For each of the three complex pier models studied here, all of the pier parameters, except Y, were kept constant. However, they are different from one model to another. In the following sections, in order to modify the existing methods in estimating b_e, the existing data from three models studied here and data from others are combined. For all of the data, h and d_{50} were chosen such that the effects of h/b_c (≥ 3.4) and b_c/d_{50} (>36) on y_s were not significant (Melville and Sutherland 1988), and the effect of pile group parameters was assumed to be negligible. For Jones Experiments (Sheppard and Renna 2005) the ratio of h/b_c is 2, but it is assumed to have negligible influence on the obtained results. Finally, Eq. (5) may be reduced to

$$\frac{y_s}{b_c} \quad \text{or} \quad \frac{b_e}{b_c} = f\left(\frac{U}{U_c} \quad \text{or} \quad \text{Fr}, \frac{Y}{b_c}, \frac{b_c}{b_{\text{pc}}}, \frac{L_U}{L_f}, k_{\text{sc}}, k_{\text{spc}}\right) \tag{6}$$

In the following sections, a summary of these nondimensional groups are presented for data of the present study and data from other researchers that were used in this study (see Table 5). Nondimensional parameters may be rearranged. For example, the parameters L_U/b_c and L_f/b_c in Eq. (5) could be replaced with L_U/L_f because, in combination, all three parameters are interchangeable.

Furthermore, in the section where we discuss the effect of pile elevation on the scour depth, data from each model (I, II, III) are analyzed separately. Since b_c/b_{pc}, T/b_{pc}, L_U/b_c, L_f/b_c, and pile group parameters are constant for each model, it can be assumed that y_s/b_c is only a function of Y/b_c. However the value of y_s depends also on the U/U_c when $Y \approx 0$, but it does not impact significantly the generality of our conclusions, as the main objective of this study is to evaluate and improve the current available methodologies in determining y_s. On the other hand, the effects of U/U_c or Fr are considered in single pier equations that are used for determining y_s by using b_e.

Experimental Setup

The experiment works were carried out in a 4.0-m-long, 0.6-m-wide, and 0.3-m-deep flume at Sharif University of Technology, which was equipped with a 13-cm-deep sediment recess through the flume. Vertical screens were placed at the leading edge of the flume to straighten the flow and generate a turbulent flow at the entrance. To ensure a developed boundary layer at the test section, located about 3 m from inlet, the most upstream 0.6 m of recess was filled with 7–14 mm gravels. The remaining recess was filled with uniform sand with d_{50}=0.6 mm and geometric standard deviation, σ_g=1.2. Two sets of experiments were conducted on the complex pier models (Fig. 1) and one set was conducted on a column-foundation combination model (Fig. 2). In this study, only rectangular piers were considered. The pier characteristics for the three models are summarized in Table 1.

The depth, h, was adjusted by the position of the sluice gate at the downstream end of the flume, and was selected to be relatively constant in the range of 14–15.5 cm, except for Experiments 2 and 3 in Table 2. The flow discharge, Q, controlled by a valve connected in the supply pipeline, was measured using a flow meter with an accuracy of ±1 L/s. A point gauge with an

Table 1. Pier-Geometry Characteristics

Model	I	II	III
$b_c(m)$	0.022	0.042	0.027
$L_c(m)$	0.15	0.15	0.09
$b_{pc}(m)$	0.09	0.09	0.05
$L_{pc}(m)$	0.18	0.19	0.10
$L_u(m)$	0.015	0.025	0.0115
$L_f(m)$	0.034	0.024	0.010
$T(m)$	0.032	0.042	—
m	3	3	—
n	2	2	—
$b_{pg}(m)$	0.016	0.016	—
$S_b(m)$	0.032	0.048	—
$S_l(m)$	0.04	0.065	—

accuracy of ±1 mm was used to measure y_s, just upstream of the pile cap where the deepest point of scour hole was found in most cases.

Pier dimensions and flow depth were selected so that the contraction effects, sediment size, and flow depth effects on y_s become negligible (Raudkivi and Ettema 1977; Melville and Sutherland 1988). To maintain the clear-water condition, the flow intensity was selected so that $0.72 \leq U/U_c \leq 0.85$ in all tests, where U_c was predicted using Shields diagram and expressions given in Melville and Coleman (2000). Also, the obtained critical shear velocity was confirmed by using alternative methods reviewed and assessed by Beheshti and Ataie-Ashtiani (2008). In addition, some experiments were conducted without pier to verify the value of U_c.

Depending on which part of the pier was exposed to the flow, one long-term experiment was carried out for each case of pier states (with top position of pile cap below, on, and above the bed).

Table 2. Results of Model I

Experiment	h/b_c	Q (L/s)	U/U_c	Y/b_c	t (h)	b_e (m)	y_s/b_c
1	6.409	19.7	0.763	3.182	10.5	0.023	1.909
2	6.136	19.7	0.800	2.727	35.5	0.019	1.682
3	6.091	19.8	0.811	2.273	15.8	0.021	1.909
4	6.636	21.3	0.791	1.818	15.8	0.020	1.727
5	6.409	21.858	0.841	0.000	36.0	0.013	1.182
6	7.091	21.78	0.750	0.000	34.5	0.018	1.500
7	6.682	21.44	0.788	0.591	54.0	0.009	0.818
8	6.909	24.1	0.851	−0.773	72.0	0.027	2.500
9	6.909	21.4	0.757	0.182	36.0	0.004	0.364
10	6.773	22.5	0.816	−0.091	75.0	0.011	1.000
11	7.000	21.2	0.742	−0.318	72.0	0.017	1.364
12	6.682	20.7	0.760	−0.318	46.0	0.028	2.364
13	6.682	20.6	0.758	−0.364	18.8	0.025	2.045
14	6.636	20.4	0.756	−0.364	18.6	0.019	1.545
15	6.773	21.9	0.794	−0.591	36.0	0.024	2.091
16	6.773	20.3	0.738	−0.636	14.3	0.025	2.045
17	6.727	20.3	0.740	−0.636	20.6	0.026	2.091
18	6.818	20.4	0.734	−0.818	16.5	0.024	1.955
19	6.909	20.4	0.722	−0.773	28.5	0.034	2.727
20	6.818	21.3	0.764	−1.045	32.5	0.033	2.727
21	7.045	21.2	0.737	−1.091	21.0	0.027	2.227
22	6.818	21.2	0.760	−1.273	34.1	0.039	3.182
23	6.773	21	0.759	−1.273	21.0	0.040	3.318
24	6.364	21	0.817	−1.773	33.4	0.023	2.091
25	6.909	20.9	0.743	−1.682	32.6	0.029	2.318
26	6.909	21.2	0.750	−1.682	21.0	0.031	2.500
27	6.909	21.1	0.749	−1.682	36.0	0.027	2.182
28	6.864	20.9	0.747	−2.091	21.4	0.028	2.318
29	6.455	20.8	0.795	−3.227	18.8	0.034	2.955
30	6.773	21.6	0.781	−5.273	33.8	0.029	2.850
31	6.727	21.5	0.785	−5.045	34.5	0.028	2.770
32	6.818	21.5	0.773	−5.045	34.1	0.036	3.016
33	6.545	21.1	0.795	−6.864	54.0	0.033	2.864
34	6.727	21.6	0.787	−7.182	15.0	0.032	2.727
35	6.455	20.6	0.792	−7.273	36.1	0.034	2.909
36	6.818	21.3	0.765	−7.500	22.7	0.033	2.727
37	7.045	20.75	0.721	−7.455	15.8	0.023	1.818
38	6.545	20.2	0.764	−8.182	19.5	0.026	2.182
39	6.455	20.2	0.773	−8.182	12.0	0.029	2.409

Table 3. Results of Model II

Experiment	h/b_c	Q (L/s)	U/U_c	Y/b_c	t (h)	b_e (m)	y_s/b_c
1	3.571	21	0.750	1.905	36.0	0.035	1.476
2	3.595	21.2	0.750	2.143	36.0	0.033	1.429
3	3.619	21.16	0.751	0.262	30.0	0.038	1.619
4	3.524	21.99	0.804	0.952	47.3	0.021	0.952
5	3.452	21.43	0.801	0.548	48.0	0.028	1.286
6	3.500	21.34	0.786	−0.571	22.5	0.045	2.000
7	3.571	21.12	0.761	−0.095	49.5	0.049	2.119
8	3.548	21.43	0.778	−0.524	34.5	0.048	2.143
9	3.548	21.46	0.777	−0.714	36.0	0.048	2.119
10	3.643	22.37	0.784	−0.833	30.8	0.041	1.833
11	3.548	21.19	0.767	−0.881	21.0	0.041	1.810
12	3.548	20.96	0.761	−1.190	36.0	0.041	1.762
13	3.595	20.92	0.748	−1.381	36.0	0.041	1.738
14	3.595	20.97	0.747	−3.071	34.5	0.032	1.357
15	3.643	21	0.740	−2.667	10.7	0.033	1.381
16	3.524	21.3	0.776	−3.048	19.5	0.028	1.238
17	3.571	21.9	0.789	−2.857	15.2	0.026	1.167
18	3.524	21	0.768	−3.214	18.2	0.022	0.976
19	3.571	21	0.758	−3.905	15.0	0.022	0.976
20	3.667	21.2	0.738	−4.405	22.5	0.023	0.952
21	3.571	21	0.77	−4.524	22.5	0.023	0.952
22	3.333	22	0.78	−4.405	22.5	0.020	0.905

These experiments were run until the rate of the development of scour hole was less than 5% of the smallest length scale of the complex pier or flow depth at 24 h (Melville and Chiew 1999). The time development of scour depth in each experiment was measured under water with no flow. After long-period experiments for each case of pier states, the other tests were run for a period of 90% of the expected maximum scour depth based on the result of the long-term experiments. In these calculations, b_e of the complex piers was considered instead of D and is calculated based on the Coleman (2005) procedure. For each test, b_e and then y_s was estimated from the slope of a trend line fitted to the resulting plot of scour depth versus the time. Using the proposed equation of Melville and Coleman (2000), y_s was described as a function of b_e and the other parameters. As described by Coleman (2005), this process was repeated until the assumed and recalculated value of b_e agreed.

Results

Effects of Pile Cap Elevation and Thickness on Scour Depth

To investigate the effects of pile cap elevation, Y, on y_s, the experiments of each model were conducted for different values of Y. The test conditions and the collected experimental data are given in Tables 2–4. Seven states based on different Y were considered (Fig. 3). Figs. 4–6 compare the variation of y_s/b_c with Y/b_c obtained from experiments and predictions by existing procedures. In these figures, $Y>0$ when the pile cap is located below the initial bed level. The numbers on these diagrams indicate which of the seven states is being considered. The variations of y_s with

Table 4. Results of Model III

Experiment	h/b_c	Q (L/s)	U/U_c	Y/b_c	t (h)	b_e (m)	y_s/b_c
1	5.481	20.1	0.76	2.593	25.5	0.028	1.889
2	5.259	21	0.79	2.222	30.0	0.024	1.667
1	5.593	21.47	0.769	0.370	34.5	0.018	1.259
2	5.444	21.46	0.789	0.000	37.5	0.026	1.852
3	5.556	21.48	0.770	−0.370	46.5	0.027	1.852
4	5.444	21.525	0.791	−0.630	36.0	0.032	2.296
5	5.444	21.52	0.791	−0.667	36.0	0.035	2.481
6	5.481	21.38	0.781	−0.815	12.0	0.030	2.074
7	5.481	21.38	0.781	−0.963	36.0	0.034	2.370
8	5.481	21.43	0.783	−1.370	36.0	0.036	2.519

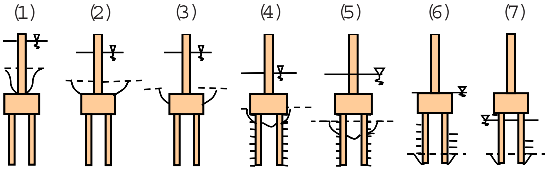

Fig. 3. Illustration of seven states for complex piers due to varied pile cap elevation

Y at the presented diagrams agree well with the given trends by the other investigators (Coleman 2005; Melville and Coleman 2000).

In Figs. 4 and 5, the first experiment in each set was conducted for the single pier (column only). This situation represents the case when the pile cap is below the base of the scour hole (Case 1 in Fig. 3). In some cases, when the scour hole reaches the top of the pile cap, the downflow and hence the horseshoe vortex induced by the column are weakened and the local scour is reduced. This process leads to an equilibrium condition (Case 2 in Fig. 3). The relative location that leads to the minimum scour depth varies for different piers. For a known condition of flow and bed sediments, this position depends on the column width and pile cap extension relative to the column. Also, the column geometry characteristics influence the beginning of scour process and its development.

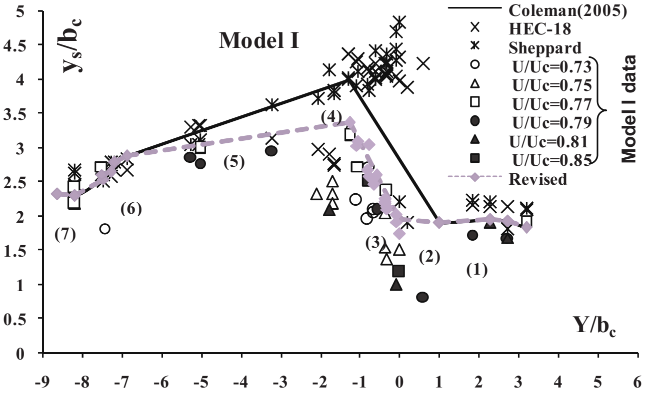

Fig. 4. Scour depth as function of Y for Model I

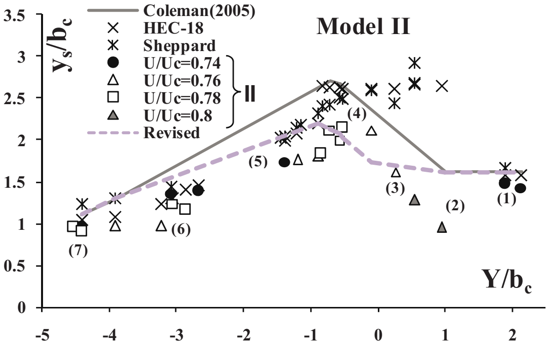

Fig. 5. Scour depth as function of Y for Model II

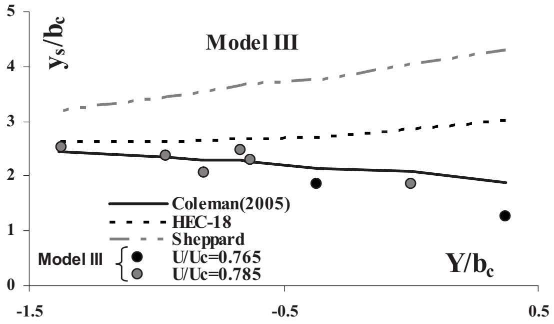

Fig. 6. Scour depth as function of Y for Model III

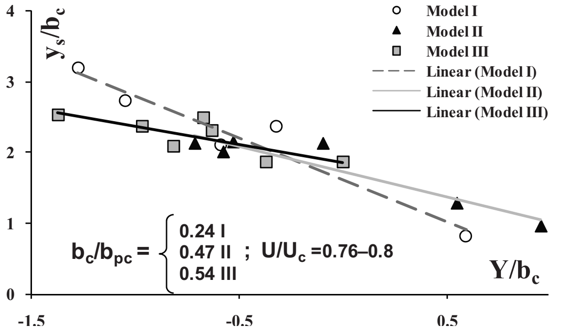

Fig. 7. Scour depth as a function of Y for different models with different b_c/b_{pc}

With increasing Y, the pile cap would be located within the local scour-hole domain and y_s increases due to the influence of the larger-diameter pile cap (Case 3 in Fig. 3), i.e., with increasing exposed surface to the flow. This process continues until the pile cap is undercut and flow penetrates below the pile cap (Case 4 in Fig. 3). In the Coleman (2005) notation, the pile cap position for undercutting was defined as Y_T. When the pile cap is undercut and all three components of pier are exposed to the flow (Case 5 in Fig. 3), y_s is reduced relative to the column-foundation combination due to the exposure of the pile group (Fotherby and Jones 1993). This reduction in y_s, for the models studied here, is due to the decreasing of the equivalent width for the complex pier subjected to the flow as the pile cap emerges from the water. Also, when the pile cap is undercut only partially (the rear portion of the pile cap is not undercut) the flow is blocked between pile groups, which leads to a reduction in y_s. With gradually increasing Y, the column is located above the water surface level. Hence, y_s depends on the characteristics of pile cap and pile groups (Case 6 in Fig. 3). This combination is similar to the case of pile groups and debris rafts as described by Melville and Dongol (1992). The influence of pile cap gradually decreases and eventually y_s reaches the same scour depth as for the pile groups (Case 7 in Fig. 3).

In addition to parameters affecting scour process around a single pier, other parameters are also important for a complex pier. Existing data between Cases 3 and 4 (without pile group effects) reveal that y_s is highly sensitive to Y. Also column-footing width ratio, b_c/b_{pc}, has a significant effect on this sensitivity. The experimental results of Melville and Raudkivi (1996) showed that for the pier and pile cap combination (Cases 3 and 4) the rate of scour variation with Y decreases when b_c/b_{pc} increases because the complex pier tends to act as a uniform pier. We have run no special experiments in this research to support particularly this idea, but comparing the slope of the trend lines fitted to the scour data (between Cases 3 and 4) could be used to illustrate this idea more clearly. Fig. 7 for Model I (with b_c/b_{pc}=0.24), Model II (with b_c/b_{pc}=0.47), and Model III (with b_c/b_{pc}=0.54) shows the differences between the rates of scour variations for the different ratios of b_c/b_{pc} with increasing Y.

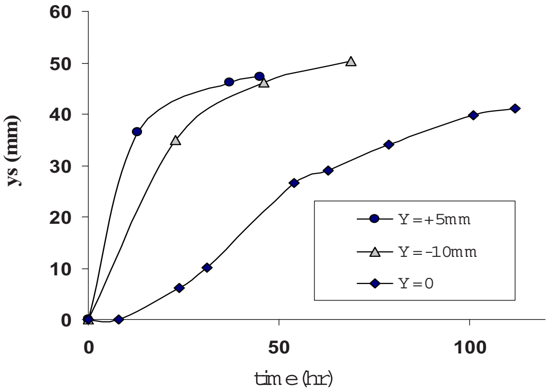

Fig. 8. Temporal development of scour depth for different values of pile cap elevation in Model I

The thickness of pile cap, T, is another effective parameter on the scour depth. Even in the cases that the pile cap is not exposed to the flow at the beginning of scouring, T could be important to determine the value of Y_T after the scour development. In addition, as mentioned by Sheppard and Glasser (2004), when the pile cap elevation is near the bed surface ($Y \approx 0$), sediment coarseness and flow intensity are more important than in other states and a minor variation in velocity and flow intensity may lead to a change in equilibrium time and scour depth.

Time Development of Scour Depth

The temporal development of the scour hole at the complex pies depends on Y (Melville and Raudkivi 1996). When $Y \approx 0$, the pile cap extensions in both directions of pier (L_u and L_f) protect the bed from scour and postpone the beginning of the scour development, and it takes a long time to achieve equilibrium conditions. Fig. 8 illustrates the time development of scouring for the three different values of pile cap elevation in Model I. For $Y \approx 0$, the initial erosion started 8 h after beginning the test at the upstream edges of pile cap. For the other values of Y, scour started and developed rapidly. Melville and Raudkivi (1996) also showed that the footing extension delayed the scour development for the cylindrical compound piers. The initial scour begins behind the pier due to the wake vortices and then it develops around the column gradually. Based on the present experiments at $Y \approx 0$, the lengths of the column and foundation play an important role in the beginning and development of scour. For $Y \approx 0$, the scour hole did not cover the pier surrounding completely (Fig. 9); rather, removed sediments from the front face deposited along pile cap toward the downstream and prevent scour from encircling the entire pier. Consequently, even though a complex pier may not be skewed to the flow, pier length is an important parameter. These results are consistent with Briaud et al. (2004).

Fig. 9. Observed scour depth at complex pier before undercutting the pile cap

Estimating Scour Depth at Complex Piers

As shown in Figs. 4 and 5 for the two first series of experiments, the maximum y_s occurred in Case 4, before the pile cap was undercut and the scour hole reached to the pile group. Consequently, it is expected that Cases 3 and 4 are critical for the scour considerations of foundation design. In order to evaluate y_s which occurs in Cases 3 and 4, we consider the data of the experiments performed by Jones at the FHWA Turner Fairbanks Laboratory (Sheppard and Renna 2005), Parola et al. (1996) data, Melville and Raudkivi (1996) data, Coleman (2005)data, and the data presented in this study. A summary of experimental conditions for data from these researchers and data at this study is reported in Table 5. In the following, some of the available methodologies for the estimation of scour depth around complex pier are applied to the present experimental data and their performances are evaluated.

Coleman's Methodology

In the Coleman (2005) procedure, it is assumed that the equivalent cylindrical-pier diameter b_e is a function of Y for a complex pier, and to predict y_s, the following equations are used in estimating a value of b_e, assuming linear variation of b_e when Y is between the given values

$$b_e = b_c \quad \text{for} \quad Y \geq b_c \tag{7}$$

$$b_e = b_c \left(\frac{b_c}{b_{\mathrm{pc}}} \right)^{\{(b_c/b_{\mathrm{pc}})^3 + 0.1 - [0.47(0.75 - Y/b_c)^{0.5}]\}} \quad \text{for} \quad Y_T \leq Y < 0 \tag{8}$$

$$b_e = \left[\frac{0.52Tb_{\mathrm{pc}} + (h - 0.52T)b^*_{\mathrm{pg}}}{h} \right] \quad \text{for} \quad Y = (-h) \tag{9}$$

Table 5. Summary of Experimental Data Used in Evolution and Improving Existing Methods

Researcher(s)	h/b_c	b_c/d_{50}	U/U_c	Y/b_c	b_c/b_{pc}	L_U/b_c	T/b_c	b_{pg}/b_c	S_b/b_{pg}
Parola et al. (1996)	2.7–8	32–97	—	−4.6 to 2	0.25–0.75	0–2.93	—	—	—
Jones Exps. (Sheppard and Renna 2005)	2	152	1.18	−0.2 to 1	0.5–0.83	0.1–0.5	0.2	—	—
Present study	3.3–7.1	37–70	0.72–0.85	−8.2 to 3.2	0.24–0.54	0.42–0.68	1–1.45	0.38–0.73	2–3
Melville and Raudkivi (1996)	4.4–20	12–188	≈1	−20–2.5	0.12–0.82	0.11–3.55	—	—	—
Coleman (2005)	3.3–7.1	37–70	0.72–0.85	−8.2 to 3.2	0.24–0.54	0.42–0.68	1–1.45	0.38–0.73	2–3

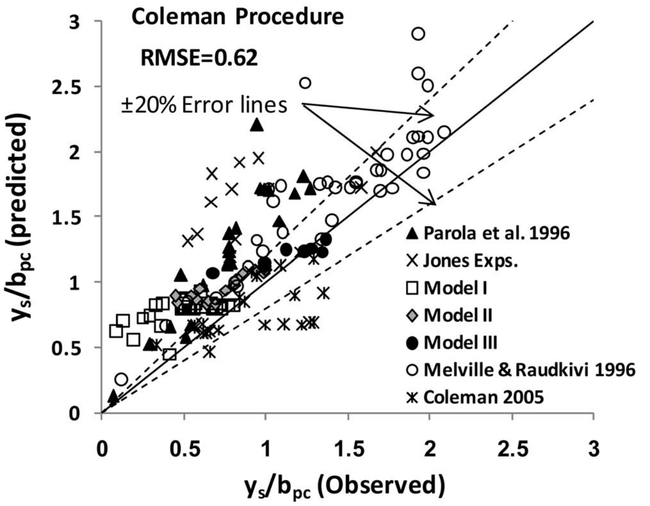

Fig. 10. Comparison of the observed and computed scour depths using Coleman (2005) procedure

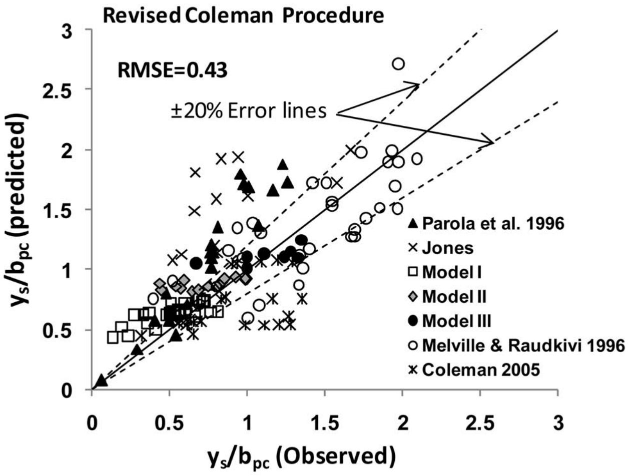

Fig. 11. Comparison of the observed and computed scour depths using revised Coleman (2005) procedure

$$b_e = b^*_{\mathrm{pg}} \quad \text{for} \quad Y \leq (-h-T) \tag{10}$$

where b^*_{pg}=equivalent width of pile group. This methodology takes advantage of the analyses of Melville and Coleman (2000) in estimating the equilibrium scour depth

$$y_s = K_{hb} K_I K_d K_s K_\alpha \tag{11}$$

where K_I=flow intensity factor, which is U/U_c for the clear-water condition ($U/U_c < 1$); K_d=sediment size factor which is equal to 1 for the present tests because $b_e/d_{50} > 25$; K_s=pier shape factor which is constant for each set of experiments; K_α=factor to account pier alignment and is equal to 1 for all tests; and K_{hb} =factor for flow depth-pier size, which is equal to $2.4b_e$ when $b_e/h < 0.7$, as in all of our tests. According to this methodology, y_s in this study is not a function of h.

As shown in Figs. 4 and 5, this procedure overestimates y_s for Models I and II, but properly reproduces the trends of collected data. Fig. 10 shows a comparison for the existing data from this study and other researchers with the computed y_s from Coleman (2005) procedure. In this figure the ±20% error lines and the line of perfect agreement are shown for comparison.

According to Figs. 4 and 5, the application of this procedure for a noncircular pier, such as Models I and II, requires some correction factors. The Coleman (2005) procedure provided reasonable result for Model III, with the same extensions of footing in two directions, and with the column-footing width ratio equal to 0.5. As shown in Figs. 4 and 5, for the present data, if y_s of the pier-foundation combination (Case 4) were estimated correctly, the scour depth for the other cases would be estimated reasonably well too. So, for the Coleman (2005) methodology only Eq. (8), which applies to pile cap and pier combination, was modified. Eq. (8) was empirically derived using the data available from the Melville and Raudkivi (1996), and is expected to give a good estimation for circular nonuniform piers. For complex piers with rectangular shapes, as stated in the previous sections, the extension of the pile cap to the upstream and the sides of the column has an important effect on scour depth. In the following, this relationship is modified for consideration of the influence of the extension of pile cap and shape factors for noncircular piers. Each group of experiments was carried out on the different models of piers. Eq. (8) was improved based on dimensionless factors that remained fixed for all the tests of each model

$$b_{eR} = k_{\mathrm{sc}} k_{\mathrm{spc}} b_e \left(1 - 0.04\left(\frac{L_U}{L_f}\right)^{1.47}\right) \times \left(\frac{b_c}{b_{\mathrm{pc}}}\right)^{0.75\{(b_c/b_{\mathrm{pc}})^3+0.1-[0.47(0.75\,-\,Y/b_c)^{0.5}]\}+0.66} \tag{12}$$

where b_e=equivalent cylindrical-pier diameter obtained from Eq. (8) and b_{eR}=modified diameter is this study. Figs. 4 and 5 compare predictions of the corrected procedure for Models I and II, with those of previous procedure. Fig. 11 shows that the computed values of y_s are reasonably close to the observed values.

Sheppard's Methodology

The scour depth predictions using the Sheppard's procedure are shown in the Figs. 4–6 for all models. This method does not properly predict the effect of buried or partially buried pile cap, overestimating y_s for Case 3. For Case 4, this method does not show any rapid reduction in y_s caused by undercutting the pile cap, but it appropriately predicts y_s at complex piers when all of the three components of pier are exposed to the flow.

HEC-18 Methodology

For the HEC-18 procedure and for all of the tests in each series, the nondimensional values of K_1, K_2, K_3, and K_4 were the same and the changes of other factors were negligible. Consequently, the value of y_s in each set changed significantly only due to the variation of Y.

The predicted data are presented in Figs. 4 and 5. As shown in these figures, the HEC-18 methodology overestimates y_s especially for Cases 3 and 4 (Fig. 3), and does not predict the variations of y_s in these cases properly. A comparison of computed versus measured y_s (Fig. 12) indicate that the HEC-18 equation overestimates most of the existing data. For the state of pier and foundation, the last part of Eq. (1) is eliminated. To correct this approach, two nondimensional factors, K_A and K_B, were obtained for the pier scour and footing scour, respectively, and derived according to Parola et al. (1996) and by using data from the present study, are suggested

$$y_{s\ \mathrm{total}} = K_A y_{s\ \mathrm{pier}} + K_B y_{s\ \mathrm{pc}} \tag{13}$$

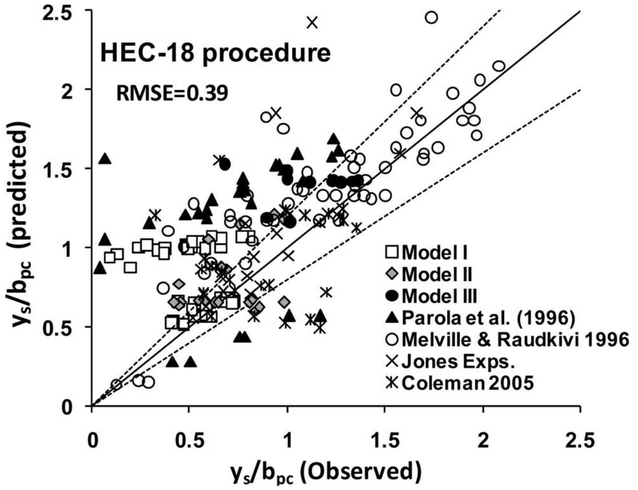

Fig. 12. Comparison of the observed and computed scour depths using HEC-18 procedure

$$K_A = 0.4(2.5 - L_U/b_c) \quad \text{for} \quad L_U/b_c \le 2.5 \tag{14}$$

$$K_A = 0 \quad \text{for} \quad L_U/b_c > 2.5 \tag{15}$$

$$K_B = \left(\frac{b_{\text{pc}}}{h_{\text{new}}}\right)^{0.1} \tag{16}$$

$$h_{\text{new}} = h + K_A y_{s\ \text{pier}} \tag{17}$$

where K_A=correction factor for the pier stem, which is related to the effect of pile cap extension on the scour depth caused by pier. For $L_U/b_c > 2.5$, according to the Parola et al. (1996) and Coleman (2005), K_A is considered to be equal to zero, therefore the scour component caused by the pier is eliminated. K_B is a correction factor for the pile cap which was selected originally based on considering the pile cap as a wide pier for estimating the scour. The computed values of the scour depths using HEC-18 procedure with new corrections are compared with the observed scour depths in Fig. 13. As shown in the figure, the factors were derived so that the new procedure provides considerable improvements in obtained results.

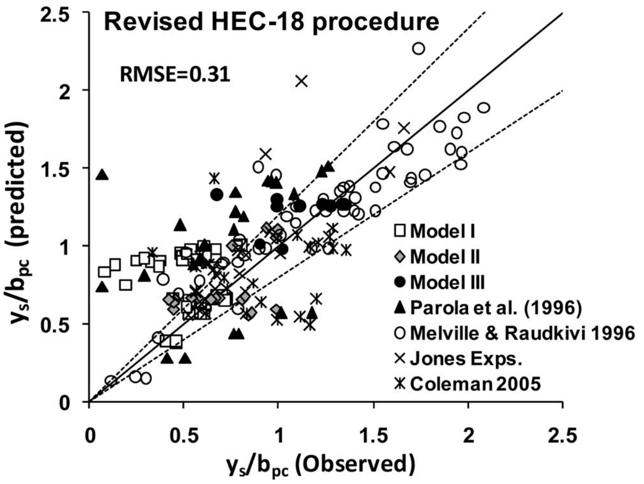

Fig. 13. Comparison of the observed and computed scour depths using revised HEC-18 procedure

Conclusions

The local scour depth of a complex pier, which is related to the components that are exposed to the flow, was studied experimentally for steady clear-water condition. A range of configurations, including the different pile cap elevations, pile sizes, and shapes of complex piers were considered. The location of pile cap that leads to the minimum scour depth (Case 2 in Fig. 3) is different for piers based on the pile cap extension and the column geometry characteristics. The maximum scour depth occurs when the pile cap was undercut. Therefore to estimate the scour depth accurately, the pile cap elevation at which the cap is undercut must be determined. However, there is not a general formula in determining of Y_T, and general prediction of Y_T needs further testing. This is highly sensitive to the pile cap elevation when the top of the pile cap is near to the bed surface and this sensitivity is more intense for smaller values of the ratio of the column width to the pile cap width. For the cases where the pile cap is located at the bed, the scour process becomes more complicated. The horizontal extensions of the pile cap protect the bed from the scour process, and due to this reason it takes a long time to reach to the equilibrium condition in these cases. With increasing pile cap elevation, the scour depth may increase or decrease dependent on the variation of the equivalent width of the complex pier subjected to the flow.

The available procedures for estimating scour depth around the complex pier were applied to the present experimental data and their performances were evaluated. In most cases, using the FHWA (HEC-18) and Coleman (2005) procedures lead to the conservative estimates of the scour depth for complex piers. Modifications were proposed to improve these methodologies so that the modified equations fit existing data better in comparison with the original procedures. Because a good prediction of Y_T for the Coleman (2005) procedure is not available, the use of a modified HEC-18 procedure is recommended. It can be inferred that this methodology is comparatively simple and practical to estimate scour depth for complex piers.

Acknowledgments

The financial assistance of the Research Office of Sharif University of Technology and Water Resources Management Organization, Ministry of Power of the Islamic Republic of Iran (Project Code No. RIV1-86048) is appreciated.

Notation

The following symbols are used in this paper:

b_c = column width;
b_e = equivalent width of pier;
b_{eR} = modified equivalent width of pier;
b_{pc} = pile cap width;
b_{pg} = pile width;
b^*_{pg} = equivalent width of pile group;
D = diameter of pier;
D^* = effective diameter;
D^*_{column} = effective diameter of column;

D^*_{pc} = effective diameter of pile cap;
D^*_{pg} = effective diameter of pile group;
D^*_{total} = total effective diameter of complex pier;
d_{16} = sediment size which 16% of sediment is finer;
d_{50} = median particle size of sediment bed;
d_{84} = sediment size which 84% of sediment is finer;
Fr = Froude number;
g = acceleration due to gravity;
h = depth of approach flow;
K_A = correction factor for pier stem;
K_B = correction factor for pile cap;
K_d = sediment size factor;
K_{hb} = flow depth-pier size factor;
K_I = flow intensity factor;
K_S = pier shape factor;
K_α = pier alignment factor;
K_1 = shape factor;
K_2 = angle of attack factor;
K_3 = dune factor;
K_4 = correction factor for size of bed material;
k_{sc} = shape factors for pier;
k_{spc} = shape factors for foundation;
L_c = column length;
L_f = transversal extension of pile cap face out from pier face;
L_{pc} = pile cap length;
L_u = longitudinal extension of pile cap face out from pier face;
m = number of piles inline with flow;
n = number of piles normal to the flow;
Q = flow discharge;
S_b = pier spacing width;
S_l = pier spacing length;
T = pile cap thickness;
U = mean velocity of the approach flow;
U_c = critical mean velocity for particle motion;
Y = pile cap elevation relative to bed level;
Y_T = pile cap elevation relative to bed level when cap is undercut;
y_s = equilibrium scour depth;
$y_{s\ \mathrm{column}}$ = scour of column stem;
y_{spc} = scour of pile cap;
y_{spg} = scour of pile group;
y_{stotal} = total local pier scour depth; and
σ_g = geometric standard deviation of particle size distribution, $\sigma_g = (d_{84}/d_{16})^{0.5}$.

References

Ataie-Ashtiani, B., and Beheshti, A. A. (2006). "Experimental investigation of clear-water local scour at pile groups." *J. Hydraul. Eng.*, 132(10), 1100–1104.

Beheshti, A. A., and Ataie-Ashtiani, B. (2008). "Analysis of threshold and incipient conditions for sediment movement." *Coastal Eng.*, 55, 423–430.

Breusers, H. N. C., and Raudkivi, A. J. (1991). *Scouring*, Balkema, Rotterdam, The Netherlands.

Briaud, J.-L., Chen, H.-C., Li, Y., and Nurtjahyo, P. (2004). "SRICOS-EFA method for complex piers in fine-grained soils." *J. Geotech. Geoenviron. Eng.*, 130(11), 1180–1191.

Coleman, S. E. (2005). "Clearwater local scour at complex piers." *J. Hydraul. Eng.*, 131(4), 330–334.

Ettema, R., Melville, B. W., and Barkdoll, B. (1998). "Scale effect in pier-scour experiments." *J. Hydraul. Eng.*, 124(6), 639–642.

Fotherby, L. M., and Jones, J. S. (1993). "The influence of exposed footings on pier scour depths." *Proc., 1993 Hydraulic Engineering Conf.*, ASCE, Reston, Va., 922–927.

Hannah, C. R. (1978). "Scour at pile groups." *Res. Rep. No. 28-3*, Dept. of Civil Engineering, Univ. of Canterbury, Christchurch, New Zealand.

Melville, B. W., and Chiew, Y. M. (1999). "Time scale for local scour at bridge piers." *J. Hydraul. Eng.*, 125(1), 59–65.

Melville, B. W., and Coleman, S. E. (2000). *Bridge scour*, Water Resources Publications, Littleton, Colo.

Melville, B. W., and Dongol, D. M. S. (1992). "Bridge piers scour with debris accumulation." *J. Hydraul. Eng.*, 118(9), 1306–1310.

Melville, B. W., and Raudkivi, A. J. (1996). "Effects of foundation geometry on bridge pier scour." *J. Hydraul. Eng.*, 122(4), 203–209.

Melville, B. W., and Sutherland, A. J. (1988). "Deign methods for local scour at bridge piers." *J. Hydraul. Eng.*, 114(10), 1210–1226.

Parola, A. C., Mahavadi, S. K., Brown, B. M., and El-Khoury, A. (1996). "Effects of rectangular foundation geometry on local pier scour." *J. Hydraul. Eng.*, 122(1), 35–40.

Raudkivi, A. J., and Ettema, R. (1977). "Effect of sediment gradation on clear water scour." *J. Hydraul. Div.*, 103(10), 1209–1213.

Raudkivi, A. J., and Ettema, R. (1983). "Clear water scour at cylindrical piers." *J. Hydraul. Eng.*, 109(3), 338–350.

Richardson, E. V., and Davis, S. R. (2001). "Evaluating scour at bridges." *Rep. No. FHWA NHI 01-001*, Federal Highway Administration, Washington, D.C.

Sheppard, D. M., and Glasser, T. (2004). "Sediment scour at piers with complex geometries." *Proc., 2004 2nd Int. Conf. on Scour and Erosion*, World Scientific, Singapore.

Sheppard, D. M., and Renna, R. (2005). *Florida bridge scour manual*, Florida DOT, Tallahassee, Fla.